Supporting Information

Vincow et al. 10.1073/pnas.1221132110

SI Materials and Methods

Detailed Fly Genotypes. Table S1 lists the detailed genotypes of the four mutants and their respective controls. The flies used for preliminary half-life analyses (Figs. S1 and S2) were three groups with intentionally diverse genetic backgrounds: w^{1118}, $PINK1^{rv}$, and *CyOActGFP*/+. Half-lives were measured separately for each group.

Liquid Chromatography and MS. Fused silica microcapillary columns of 75 μm inner diameter (Polymicro Technologies) were packed in-house by pressure loading 30 cm Jupiter 90 Å C12 material (Phenomenex). Kasil (PQ Corporation) frit microcapillary column traps of 100 μm inner diameter with a 2-mm Kasil frit were packed with 4 cm Jupiter 90 Å C12. An equal molar mix of a six-protein bovine digest (Michrom Bioresources) was used to assess quality of the column before and during analysis. Three of these quality control runs were analyzed before any sample analysis, and another quality control run was performed after every six sample runs. Two analytical replicates were obtained for each sample; 2 μg of each sample digest and 200 femtomoles of six-protein bovine digest were loaded onto the trap and column by the NanoACQUITY ultra performance liquid chromatography (UPLC) system (Waters Corporation). Buffer solutions used were water and 0.1% formic acid (buffer A) and acetonitrile and 0.1% formic acid (buffer B). The 60-min gradient of the six-protein bovine digest quality control consisted of 40 min of 95% buffer A and 5% buffer B, 1 min of 68% buffer A and 32% buffer B, 5 min of 20% buffer A and 80% buffer B, and 14 min of 95% buffer A and 5% buffer B at a flow rate of 0.25 μL/min. The 240-min gradient for the sample digest consisted of 200 min of 95% buffer A and 5% buffer B, 1 min of 68% buffer A and 32% buffer B, 19 min of 20% buffer A and 80% buffer B, and 20 min of 95% buffer A and 5% buffer B at a flow rate of 0.25 μL/min. Peptides were eluted from the column and electrosprayed directly into an LTQ-Orbitrap mass spectrometer (Thermo Fisher) with the application of a distal 3 kV spray voltage. For the six-protein bovine digest quality control analysis, a cycle of one 30,000 resolution full-scan mass spectrum (400–1,400 m/z) was followed by six selected reaction monitoring spectra analyzing six peptides and four to five fragment ions per peptide at 35% normalized collision energy with a 2-m/z isolation window. For the sample digests, a cycle of one 60,000 resolution full-scan mass spectrum (400–1,400 m/z) was followed by five data-dependent MS/MS spectra at 35% normalized collision energy with a 3-m/z isolation window. Applications of the mass spectrometer and UPLC solvent gradients were controlled by the Thermo Fisher XCalibur data system.

Analysis of MS Data. High-resolution MS data were processed by BullsEye to optimize precursor mass information (1). The MS/MS output was searched using SEQUEST (2), with differential modification search of 3.0188325 Da for leucine and a static modification of 57.021461 Da for cysteine, against a FASTA database containing all of the protein sequences from FlyBase (10/03/09) plus contaminant proteins. Peptide-spectrum match false discovery rates were determined using Percolator (3) at a threshold of 0.01, and peptides were assembled into protein identifications using an in-house implementation of IDPicker (4).

Topograph Analysis Parameters for Half-Life Measurement. The following Topograph quality control cutoffs were applied to all data points (values of percent newly synthesized) for both half-life and abundance analyses.

i) Deconvolution score ≥0.95. The deconvolution score reflects the fit of the calculated isotopolog distribution to the observed distribution.
ii) Average turnover score ≥0.98. The average turnover score reflects the validity of precursor pool enrichment calculations.
iii) Total area under the curve (AUC) of ≥1,000,000 signal units. Data points with AUC values below this threshold generally had an unacceptable signal-to-noise ratio.

For half-life analysis, we also excluded data points more than 2 SDs above or below the protein mean for that condition (genotype and time point). Preliminary observations had shown that most such outliers were caused by artifacts, such as peak misidentification.

Topograph's retention time alignment feature was used to identify peptides in replicates where they were not detected in the MS2 spectra. In a small percentage of cases (5–7%), Topograph grouped peptides derived from a single protein into two to three nonoverlapping isoform groups, each of which was treated as a separate protein.

Calculation of Total Protein Abundance. We used Topograph to calculate total abundance for each mitochondrial protein. Topograph computes half-lives using AUC measurements to compare the abundance of the various labeled and unlabeled forms of a peptide, and therefore can measure total abundance by summing AUC for all forms of a peptide. Abundance was measured for individual peptides, because the range of absolute peptide abundances within a protein can be large. Abundance values were normalized by dividing by the sum of all abundance values in that biological replicate. For each peptide, we computed mean abundance at 240 and 120 h and used the 240-h/120-h abundance ratio as a measure of change. We then grouped the peptide results by protein and performed paired sample t tests comparing abundance ratios in mutant and control flies. Significant differences in mean abundance ratio were considered to reflect significantly different patterns of abundance over time. The P values were adjusted for multiple comparisons using the Benjamini–Hochberg step-up false discovery rate–controlling procedure with a false discovery rate of 5% (5). In the three datasets containing a few proteins with significantly different patterns of abundance between genotypes, data were reanalyzed excluding these proteins. Their absence did not significantly affect the overall results, described in *Materials and Methods*, and these proteins were therefore retained in the main analyses.

1. Hsieh EJ, Hoopmann MR, MacLean B, MacCoss MJ (2010) Comparison of database search strategies for high precursor mass accuracy MS/MS data. *J Proteome Res* 9(2):1138–1143.
2. Ducret A, Van Oostveen I, Eng JK, Yates JR, 3rd, Aebersold R (1998) High throughput protein characterization by automated reverse-phase chromatography/electrospray tandem mass spectrometry. *Protein Sci* 7(3):706–719.
3. Käll L, Canterbury JD, Weston J, Noble WS, MacCoss MJ (2007) Semi-supervised learning for peptide identification from shotgun proteomics datasets. *Nat Methods* 4(11):923–925.
4. Zhang B, Chambers MC, Tabb DL (2007) Proteomic parsimony through bipartite graph analysis improves accuracy and transparency. *J Proteome Res* 6(9):3549–3557.
5. Benjamini Y, Hochberg Y (1995) Controlling the false discovery rate: A practical and powerful approach to multiple testing. *J R Stat Soc Series B Stat Methodol* 57(1): 289–300.

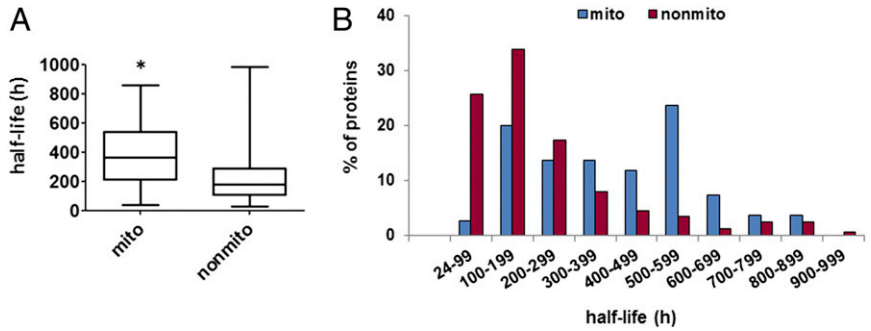

Fig. S1. Half-lives of *Drosophila* mitochondrial proteins are diverse and tend to be longer than half-lives of nonmitochondrial proteins. (*A*) Mean half-life in hours of mitochondrial and nonmitochondrial proteins (n = 160 mito; n = 364 nonmito). Box plots depict the median and the upper and lower quartiles; whiskers represent extreme values. *$P = 2.7 \times 10^{-7}$ by t test. (*B*) Histogram of half-lives for mitochondrial (blue) and nonmitochondrial (red) proteins.

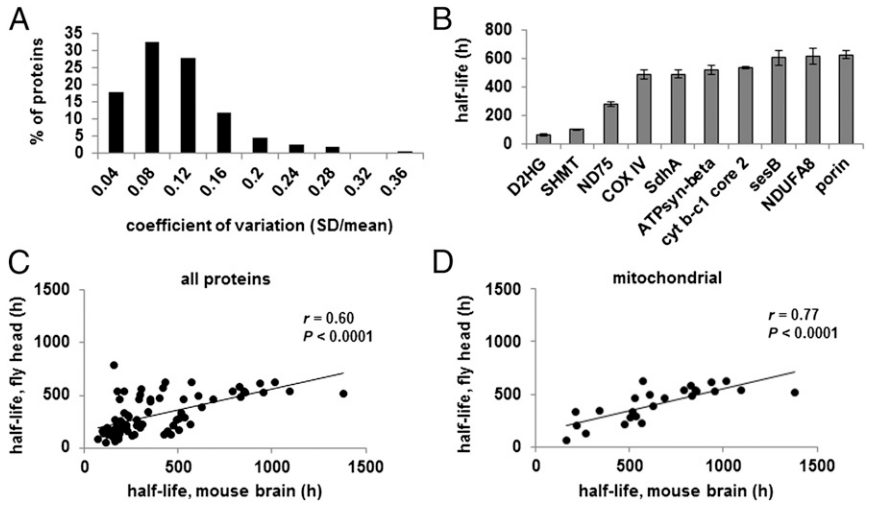

Fig. S2. Protein half-lives are reproducible across fly genotypes and are evolutionarily conserved. (*A*) Histogram of the coefficients of variation for the half-lives of proteins (n = 201) detected in flies with three different genetic backgrounds. (*B*) The mean half-lives (± SD) of 10 representative *Drosophila* mitochondrial proteins from the analysis in *A*. ATPsyn-β, ATP synthase β-subunit; COX IV, cytochrome C oxidase polypeptide IV; cyt b-1 core 2, cytochrome *b-c1* complex core protein 2; D2HG, D2-hydroxyglutarate dehydrogenase; ND75, NADH:ubiquinone reductase 75 kD subunit precursor; NDUFA8, NADH dehydrogenase (ubiquinone) 1 α-subcomplex, 8; SdhA, succinate dehydrogenase A; sesB, stress-sensitive B; SHMT, serine hydroxymethyltransferase. (*C*) Half-lives of proteins in fly heads vs. their orthologs in mouse brain. All fly proteins from Dataset S1 with orthologs in the data of Price et al. (1) were included (n = 75). (*D*) Half-lives of mitochondrial proteins in fly heads vs. their orthologs in mouse brain (n = 25).

1. Price JC, Guan S, Burlingame A, Prusiner SB, Ghaemmaghami S (2010) Analysis of proteome dynamics in the mouse brain. *Proc Natl Acad Sci USA* 107(32):14508–14513.

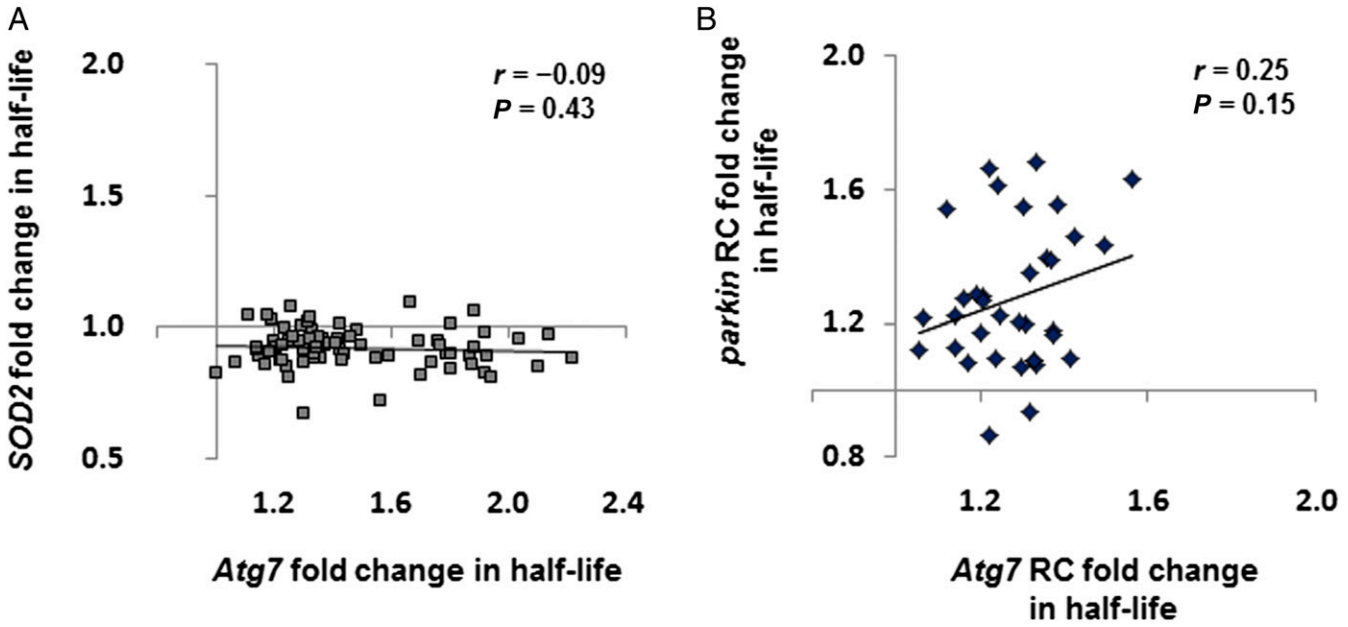

Fig. S3. Additional mutation effect comparisons for *Atg7*. (*A*) The effects of *Atg7* mutation on mitochondrial protein half-life do not correlate significantly with the effects of superoxide dismutase 2 (SOD2) deficiency ($n = 103$). (*B*) *parkin* effect on half-life does not correlate significantly with *Atg7* effect for individual respiratory chain (RC) proteins ($n = 36$).

Table S1. Detailed fly genotypes for mutant/control comparisons

Dataset	Mutant	Control	Comments
parkin	*If/CyO ; park^{25}/ park^{25}*	*If/CyO ; park^{25}/ park^{rvA}*	
Atg7	*Atg7^{d4}/Atg7^{d77}*	*Atg7^{d4}/CyOGFP* and *Atg7^{d77}/CyOGFP*	Sibling controls
PINK1	*PINK1^{B9}/Y*	*PINK1^{rv}/Y*	
SOD2	*SOD2^{n283}/SOD2^{wk}*	*CyOActGFP/+*	Sibling controls

Table S2. Mean fold change in half-life with and without proteins showing differential abundance change (DAC)

	parkin		*Atg7*		*PINK1*		*SOD2*	
	All proteins	DAC excluded	All proteins	DAC excluded	All proteins	DAC excluded	All proteins	DAC excluded
All mito proteins								
Mean ± SD	1.30 ± 0.22	1.29 ± 0.22	1.47 ± 0.30	1.48 ± 0.30	1.04 ± 0.16	1.05 ± 0.16	No DAC	No DAC
n	156	151	170	165	147	146		
Non-RC mito								
Mean ± SD	1.30 ± 0.23	1.29 ± 0.23	1.54 ± 0.31	1.54 ± 0.31	0.99 ± 0.13	0.99 ± 0.13		
n	114	109	127	124	102	101		
RC								
Mean ± SD	1.29 ± 0.20	1.29 ± 0.20	1.27 ± 0.12	1.27 ± 0.12	1.17 ± 0.16	1.17 ± 0.16		
n	42	42	43	41	45	45		

There was no significant alteration in any mean fold change value after exclusion of proteins showing differential abundance change between mutant and control (Student *t* test, *P* = not significant).

Table S3. Mutation effect correlations with and without proteins showing DAC

	parkin vs. *Atg7*		*PINK1* vs. *parkin*		*PINK1* vs. *Atg7*		*SOD2* vs. *parkin*		*SOD2* vs. *Atg7*	
	All proteins	DAC excluded	All proteins	DAC excluded	All proteins	DAC excluded	All proteins	DAC excluded	All proteins	DAC excluded
All mito proteins										
r	0.37	0.36					−0.02	−0.001	−0.07	−0.10
n	147	137					103	98	103	98
P	<0.0001	<0.0001					0.87	0.99	0.46	0.32
Non-RC mito										
r	0.42	0.40	0.45	0.47						
n	111	103	94	98						
P	<0.0001	<0.0001	<0.0001	<0.0001						
RC										
r	0.25	0.23	0.84	0.84	0.12	0.10				
n	36	34	36	36	34	32				
P	0.15	0.20	<0.0001	<0.0001	0.50	0.58				

There was no significant alteration in any reported correlation after exclusion of proteins showing differential abundance change between mutant and control (Fisher *r*-to-*z* test, *P* = not significant).

Other Supporting Information Files

Dataset S1 (XLSX)
Dataset S2 (XLSX)
Dataset S3 (XLSX)